Design, Simulation of Low Actuation RF MEMS Shunt Switches With Electromagnetic Characterization

Suraj Gaonkar
M.Tech Scholar
Department of Electronics and Communication
M.S.Ramaiah Institute of Technology
Bengaluru
surajgaonkar88@gmail.com

Lakshmi .S
Associate professor, Department of E & C
M.S.Ramaiah Institute of Technology
Bengaluru
lakshmi_ramesh@msrit.edu

***Abstract*—** Micro Electro Mechanical Systems (MEMS) is an integration of sensors, actuators, microstructures and microelectronics. Components of MEMS that comprises of moving sub milli-meter sized parts, capable of providing Radio Frequency (RF) functionality are collectively referred as RF MEMS. In this work, low actuation RF MEMS switches have been designed and simulated and they have also been analysed for electromagnetic characterization. The switches so analyzed show an actuation voltage of as low as 2V. The electromagnetic analysis gives an isolation of as high as 55-65dB and a very low insertion loss of 0.01dB.

Keywords*—Low actuation, RF MEMS switches, insertion loss, isolation.*

*****

I. INTRODUCTION

RF MEMS switches offer a substantially higher performance than PIN or Field effect transistor (FET) diode switches and have been extensively in state-of-art MEMS phase shifters & switching network up to 120GHz. In RF MEMS technology there are important issues such as long and short term reliability , packaging techniques and their effect on reliability and production cost are presently been addressed[1]. Advancement of micro fabrication techniques aided the development of MEMS in various engineering fields [2]. MEMS technology plays an important role in fabrication of RF components such as switches, variable capacitor and variable inductors. These RF components proved to be much more reliable and feasible than electrical counterparts for communication applications [3-4]. RF MEMS switches constitute a major part of RF MEMS components fabricated through batch fabrication process. RF MEMS switches have a thin metal membrane which would be actuated using electrostatic, piezoelectric, magneto static and thermal designs [5-9]. For electrostatic actuation, a dc voltage is applied between membrane and the electrodes. The membrane deflects due to electrostatic force and based on switch used, it either short circuits or open circuits transmission lines. RF MEMS have many advantages like high linearity, low dc power consumption, low insertion loss, and high isolation loss over conventional components [11-14]. Electromagnetic analysis calculates electric field, the magnetic field and their interactions at all points in space, which gives Scattering-parameters. S-parameters are expressed in terms of the power relation between input and output terminals

All RF MEMS switches that are developed are bound to follow some basic mechanical laws. In MEMS Switch, surface forces and viscous air damping dominates over inertial and gravitational forces. RF MEMS switches are classified as shown below

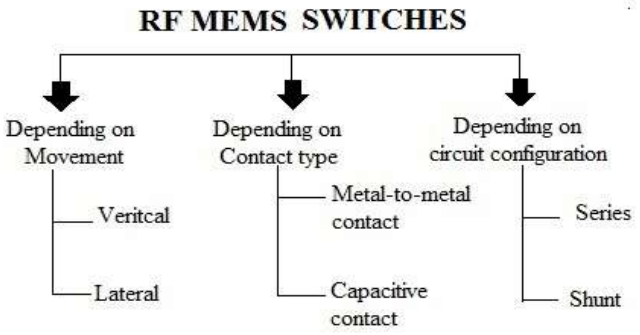

Authors in [15] have proposed electrostatically actuated switch with parallel beam configuration is proposed in which they are able to achieve a actuation voltage of 6.2V. Authors in [17] have proposed two electrostatically actuated switch with beam configuration of square serpentine flexures with pull-in voltage of 8.5V and circular serpentine flexures with pull-in voltage of 10.25V. Authors in [7] have proposed an electrostatically actuated switch with fixed-fixed beam witch circular holes and they are able to achieve a low voltage as 4V. Authors in [18] have proposed a serpentine flexure beam with AlN (aluminium nitride) dielectric layer and they are able to achieve an actuation voltage of 4V.

This paper proposes very low actuation RF capacitive switch to be compatible with the integration circuits for RF front end. In this paper three beam configuration have been proposed such as fixed-fixed beam, fixed-fixed flexures beam and crab-leg flexures.

II. FABRICATION PROCESS FLOW FOR THE PROPOSED SWITCH

The Fig. 1 gives the process step for the fabrication process for all the designed capacitive shunt switch consists of substrate layer made up of silicon material 50µm thick[16]. A stack material of thermal dioxide of 1µm is laid over the substrate over which a 0.5µm thin chromium layer is sputtered. This thin chromium layer helps the adhesion of CPW gold

layer to the substrate. Now a gold layer is sputtered to form the CPW. Now using the CPW mask the final CPW is formed. A silicon nitride layer is deposited over the CPW and then masked using the nitride mask. This forms the dielectric layer to avoid meta-metal contact between CPW and beam. A sacrificial layer photoresist is used the material used is BPSG of 3µm thickness. This forms the Gap between the beam and CPW. Now a gold layer is planar filled over the BPSG layer of 0.5µm thick which is masked using beam mask. The holes are made on the beam using the square mask. Delete step removes the sacrificial layer BPSG by etching the holes in the beam helps in the release process.

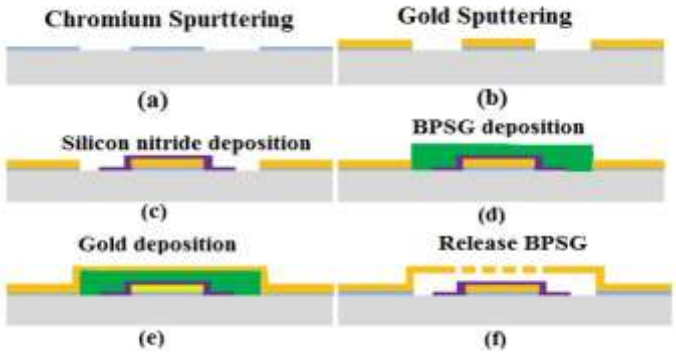

Fig.1 Fabrication process steps

III. PROPOSED RF MEMS SWITCHES

MEMS shunt switches are designed and analyzed in a FEM Tool namely Coventorware the RF characteristics have been obtained using ANSOFT HFSS. For electrostatic actuation, a dc voltage is applied between the top membrane and the electrodes. The membrane deflects due to electrostatic force and based on switch used, it either short circuits or open circuits transmission lines.

When the applied voltage between the beam and CPW signal line, equal and opposite charges develops at faces. These opposite charges generate attractive electrostatic forces causing the beam to bend towards the CPW signal line .As the beam bends, electrostatic forces which are inversely proportional to the gap increase. The mechanical restoring force is linear function of the beam displacement. Finally the beam settles to an equilibrium position. If the applied voltage increases beyond a critical value i.e $2/3g_0$, the beam becomes instable, the electric field force cannot be balanced by the elastic restoring force of the beam and the beam collapses onto the CPW signal line. The voltage and deflection at this state are known as the pull-in voltage and pull-in deflection, which are of utmost importance in the design of MEMS devices.

Under electrostatic actuation, the pull-in voltage is given by

$$V_p = \sqrt{\frac{8kg_0^{\,3}}{27\varepsilon_0 A}} \qquad (1)$$

Where 'k' is the spring constant of the beam. 'g_0' is the air gap between beam and CPW. 'A' is the actuation area between beam and CPW signal line.

a) Fixed-Fixed beam

MEMS capacitive shunt fixed-fixed beam switch is shown in figure 2. The material used for both CPW and beam is gold. The CPW is fabricated by sputtering a thin layer gold. The width of the CPW signal line 120µmX120µm. The beam length is 90µm, width is 120µm and thickness is 0.5µm.The dielectric layer of 200nm is place on the signal line of CPW. Here in this model the faces of the beam anchor are fixed, such that they do not change the position during the application voltage. The holes are added to the beam help the release process of sacrificial layer and to improve performance of the switch by reducing the stiffness of the gold beam.

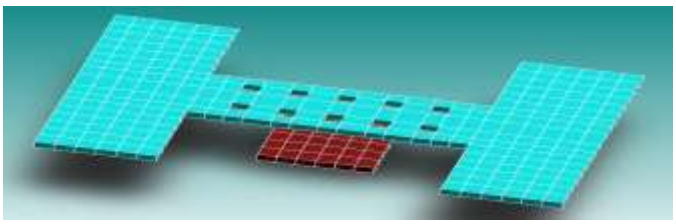

Fig.2 Fixed-Fixed beam with holes

b) Fixed-Fixed flexures beam

A MEMS capacitive shunt fixed -fixed flexures switch has a lower spring constant than the fixed-fixed beam .Hence the stiffness of the beam decreases and the pull-in voltage decreases as compared to fixed-fixed beam. The material used for both CPW and beam is gold. The CPW is fabricated by sputtering a thin layer gold. The width of the CPW signal line 120µmX120µm. The beam length is 90µm, width is 120µm and thickness is 0.5µm.The dielectric layer of 200nm is placed on the signal line of CPW. Here in this model the faces of the beam anchor are fixed, such that they do not change the position during the application voltage. The holes are added to the beam help the release process of sacrificial layer and to improve performance of the switch by reducing the stiffness of the gold beam.

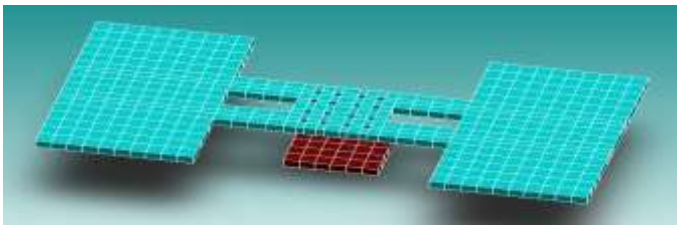

Fig.3 Fixed-Fixed flexures beam with holes

c) Crab-leg flexures beam

A MEMS capacitive shunt crab-leg flexures switch has lower spring constant than the fixed-fixed flexures beam.

Hence pull-in voltage decreases considerably. The material used for both CPW and beam is gold. The CPW is fabricated by sputtering a thin layer gold. The width of the CPW signal line 120µmX120µm.The beam anchor width is 30µm and thickness is 0.5µm.The dielectric layer of 200nm is placed on the signal line of CPW. Here in this model the faces of the beam anchor are fixed, such that they do not change the position during the application voltage.

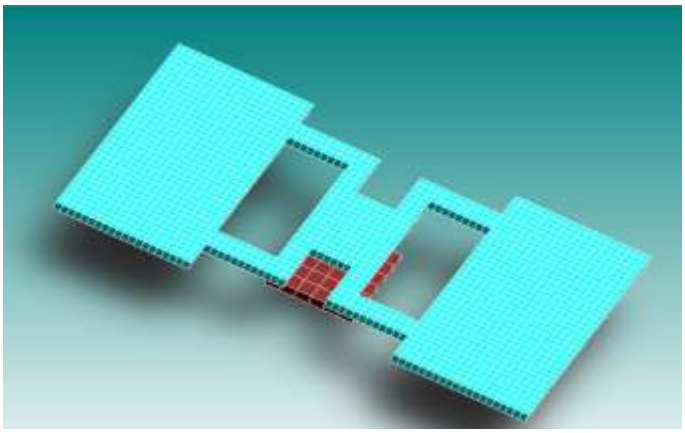

Fig.4 Crab-leg flexures beam

IV. ELECTRICAL MODEL AND DESIGN

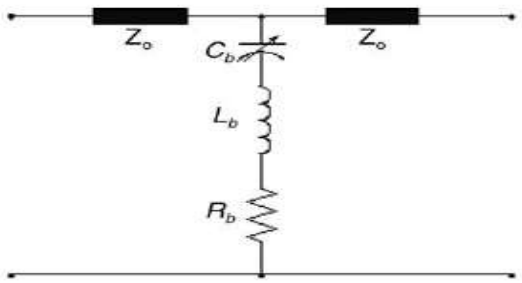

Fig.5 Equivalent circuit

Fig.2 shows the schematic of a typical RF MEMS capacitive switch, which is constructed based on a coplanar waveguide (CPW) transmission line. The switching element consists of a thin metallic bridge suspended over the centre conductor and fixed at both ends of the ground conductors of the CPW line. In this set-up, the bridge and the CPW centre conductor serve as top and bottom electrodes of a parallel-plate capacitor, respectively. Since the bridge is allowed to move freely, the parallel-plate capacitance can be increased by shortening the distance of the separation. This is done by v applying a DC bias voltage between the bridge and the center conductor of the CPW line. The DC potential generates an electrostatic force that pulls the bridge towards the center conductor, thereby decreasing the distance of the separation and increasing the capacitance. A thin dielectric layer deposited over the bottom electrode prevents stiction when the metal surfaces come into contact. [15] The RF performance of the switch is quantified by its insertion loss, return loss and isolation. Basically, it is desirable to have a low insertion loss and high return loss and isolation. In order to improve the RF performance, it is necessary to modify the bridge design of the switch. The RF capacitive switch can be modelled by a transmission line with characteristic impedance, Z_0, and a lumped series resistor–inductor–capacitor model of the bridge, as shown in Fig. 5. The metallic bridge of the switch is represented mainly by the bridge resistance R_b, bridge inductance L_b, and variable bridge capacitance C_b. The variable bridge capacitance changes according to the actuation state of the switch. Hence, the capacitor has both up-state/down-state capacitance values. The impedance of the bridge, Z_b, as seen by the centre conductor of the CPW line, is therefore given by

$$Z_b = R_b + j\left(\omega L_b - \frac{1}{\omega C_b}\right) \tag{2}$$

Where, $C = C_u$ or C_d, depending on the actuation state of the RF capacitive switch; C_u is the up-state capacitance, and C_d is the down-state capacitance. The total impedance of the switch will change with frequency because the impedance of each reactive component changes with frequency. When $\omega L_b = 1/\omega C_b$, the LC series circuit resonates. The resonant frequency, f_0, is given by

$$f_0 = \frac{1}{2\pi\sqrt{L_b C_b}} \tag{3}$$

When the switch is un-actuated, the up-state capacitance is very small and bridge inductance and resistance can be neglected. Therefore, the insertion loss, S_{21}, can be expressed as

.

$$S_{21}\,|_{f \ll f_0} = 20\log\left|\frac{1}{2 + j\omega C_u Z_0}\right| \tag{4}$$

Since the current will pass through the bridge from the CPW centre conductor to the two ground conductors when the switch is actuated, the equivalent electrical model for the resistance of the bridge is actually a pair of resistors parallel to each other. The bridge resistance of the switch, can be expressed as

$$R_b = \frac{1}{2}\frac{\rho_b\left(\frac{l_b}{2}\right)}{A_{e(b)}} \tag{5}$$

where, ρ_b is the resistivity of the bridge, l_b represents the length of the bridge, and $A_{e(b)}$ is the effectively cross-sectional area of the bridge.

At resonance, the transmission line is loaded with bridge resistance alone and the isolation of the switch is given by

 ISSN: 2321-8169
3912 - 3918

$$S_{21}|_{f_0} = 20\log\left|\frac{2R_b}{2R_b + Z_0}\right| \quad (6)$$

Therefore, the series resonance is very beneficial to the isolation performance of the shunt switch. However, this high isolation can only be achieved around the LC resonant frequency of the switch. When $f>>f_0$, the isolation is expressed as

$$S_{21}|_{f>>f_0} = 20\log\left|\frac{2j\omega L_b}{2\omega L_b + Z_0}\right| \quad (7)$$

Hence the electrical parameters of the bridge, R_b, L_b, C_u and C_d can be extracted using equation (3) to (7) from the simulated or measured *S*-parameters. Based on the electrical model analysis, if the series LC resonance of the switch occurs at X-band frequencies in the down-state, bridge resistance is the only factor that determines the isolation of the switch where the isolation will considerably increase at X-band frequencies. As indicated by equation (3), it is possible to propose two ways to reduce the resonant frequency. First method is to increase the downstate capacitance, C_d, of the bridge, which can be realized by increasing the overlapping area between the bridge and the dielectric layer. The second method is to increase the series inductance of the bridge, L_b, which can be realized by changing the geometry of the connecting beams of the bridge between the centre conductor and the ground conductor of CPW line. This is because the connecting beams mainly determine the bridge inductance. As a result, after taking into account these factors, a single-bridge switch with different beam configuration is proposed.

V. RESULTS AND DISCUSSION

A. *Fixed-Fixed beam*

Fig 6 shows the analysis of the structure after actuation of the switch. The colors show the magnitude of displacement, as it can be seen that the maximum displacement is at the center of the beam with red color. It also shows the structure of the switch when the pull-in occurs. Pull-in voltage achieved here is 3.75V.

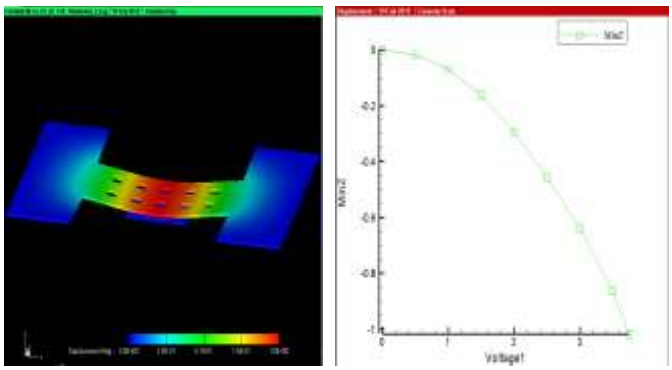

Fig.6 pull-in simulation results for fixed-fixed beam switch

Design	Beam Width	Gap 2.2µm	Gap 2.5µm	Gap 2.75µm	Gap 3µm
Fixed-Fixed beam	100µm	4.25V	5.5V	5.75V	6V
Fixed-Fixed beam	120µm	3.75V	5.5V	5.75V	6.25V

Table 1: Gap Vs Pull-in voltage

The table 1 shows that as the gap between the CPW signal line and beam increases the actuation voltage also increases.

To characterize the above structure for its RF performance, the fixed-fixed beam model is imported from the COVENTOREWARE tool into the HFSS tool as shown in Fig 7. Parametric analysis has been performed for the above structure by varying gap, beam width and actuation area.

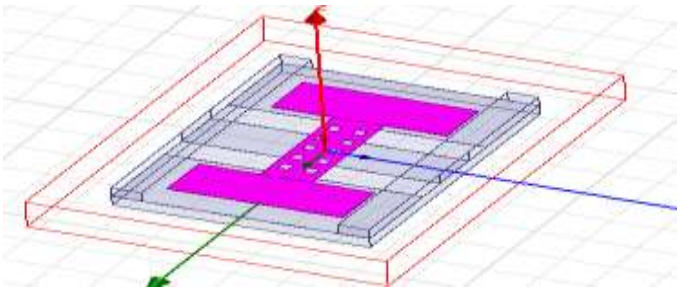

Fig. 7 Switch structure in ANSOFT HFSS

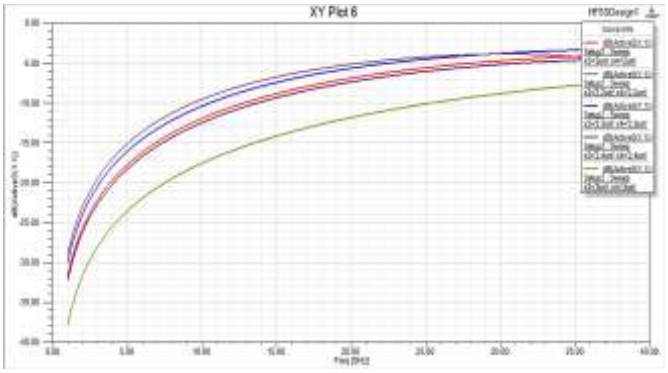

Fig.8 Return loss for fixed-fixed beam for different width in upstate position

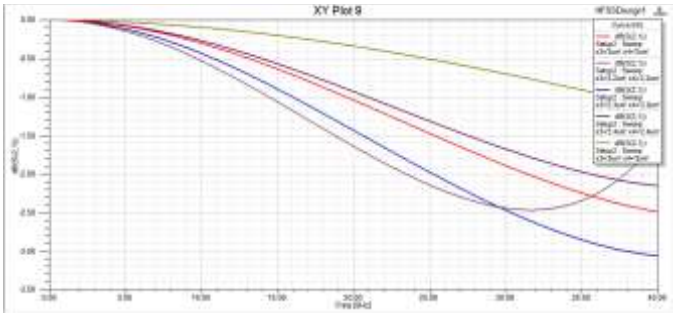

Fig.9 Insertion loss for fixed-fixed beam with different width in up-state position

 ISSN: 2321-8169
3912 - 3918

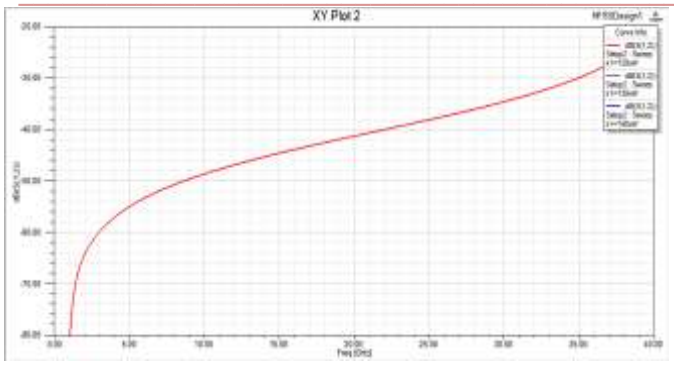

Fig.10 Isolation for fixed-fixed beam in down-state position

B. *Fixed-Fixed Flexures*

Fig 11 shows the analysis of the structure after actuation of the switch. The colors show the magnitude of displacement, as it can be seen that the maximum displacement is at the center of the beam with red color. It also shows the structure of the switch when the pull-in occurs. In fixed-Fixed flexures beam the stiffness of the beam is reduced in this structure and pull-in voltage achieved is 3.125V.

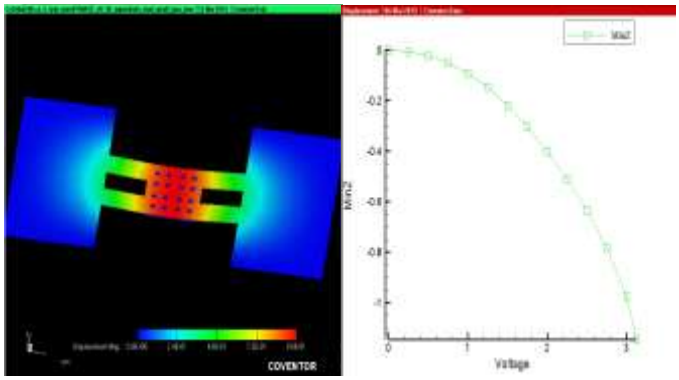

Fig.11.Pull-in simulation results for fixed-fixed flexures beam

Table 1 Pull-voltage Vs Anchor width

DESIGN	*Anchor Width(w) in µm*	*Anchor Length(l) in µm*	*Pull-in Voltage Vp*
Fixed-fixed flexures without holes	30	90	3V
Fixed-fixed flexures square holes	30	90	3.125V
Fixed-fixed flexures without holes	40	90	3.125V
Fixed-fixed flexures square holes	40	90	3.3V
Fixed-fixed flexures without holes	50	90	3.875V
Fixed-fixed flexures square holes	50	90	4.25V

Table 1 gives the values of actuation voltage for different anchor width of fixed-fixed flexures beam it can be seen that with increase in anchor width increase the actuation voltage for the switch and by adding holes the pull-in voltage is increased.

To characterize the above structure for its RF performance, the fixed-fixed flexures beam model is imported from the COVENTOREWARE tool into the HFSS tool as shown in Fig 12. Electromagnetic analysis has been performed for the above structure by varying gap, anchor width and actuation area.

.

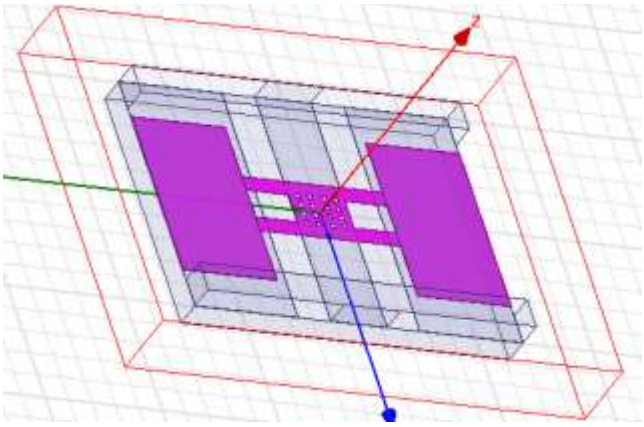

Fig.12 Switch structure in ANSOFT HFSS

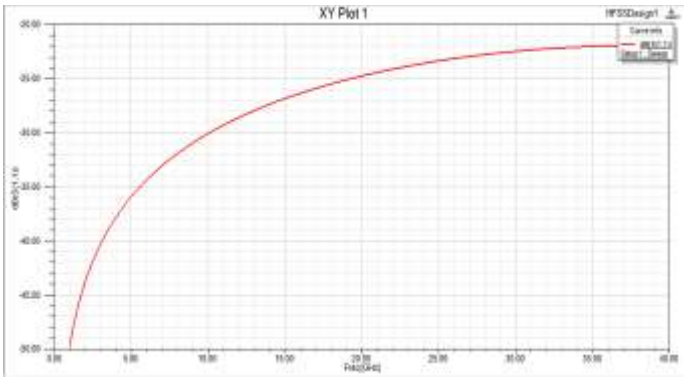

Fig.13 Return loss for fixed-fixed flexures beam in upstate position

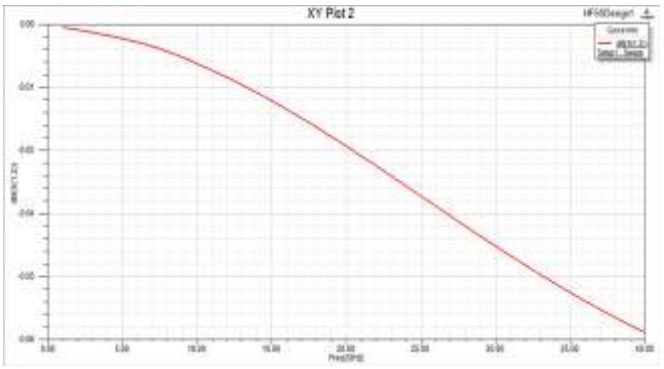

Fig.14 Insertion loss for fixed-fixed flexures beam in up-state position

 ISSN: 2321-8169
3912 - 3918

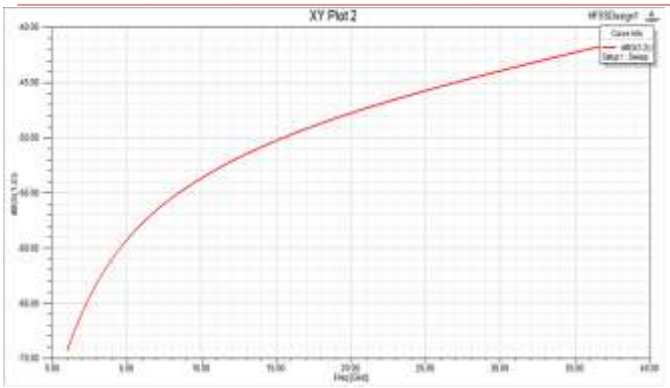

Fig.15 Isolation for fixed-fixed flexures beam in down-state position

C. *Crab-leg flexures beam*

Fig 16 shows the analysis of the structure after actuation of the switch. The colors show the magnitude of displacement, as it can be seen that the maximum displacement is at the center of the beam with red color. It also shows the structure of the switch when the pull-in occurs. In Crab-leg flexures beam the stiffness of the beam is reduced in this structure and pull-in voltage achieved is 2V.

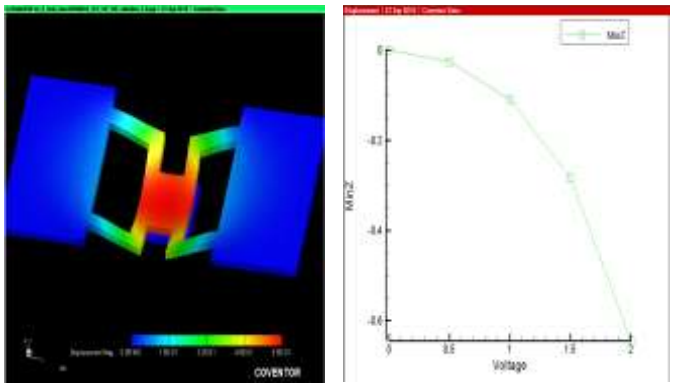

Fig.16 Pull-in simulation results for crab-leg flexures beam

Table 2 Pull-voltage Vs Actuation area

Design Name	Actuation area in μm^2	Anchor width in µm	Gap in µm	Pull-in voltage
Crab-leg flexures	100X100	30	2.2	2.25V
Crab-leg flexures	120X120	30	2.2	2V

Table 2 shows that as the actuation area increases Pull-in decreases because the pull-in voltage is inversely proportional to the actuation area.

To characterize the above structure for its RF performance, the crab-leg flexures beam model is imported from the COVENTOREWARE tool into the HFSS tool as shown in Fig 17. Electromagnetic analysis has been performed for the above structure by varying actuation area.

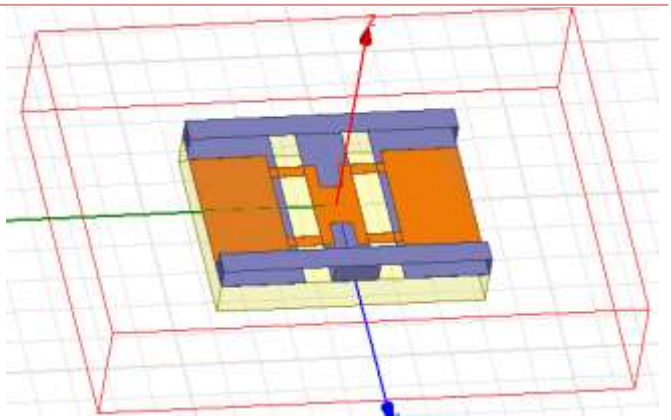

Fig.17 Switch structure in ANSOFT HFSS

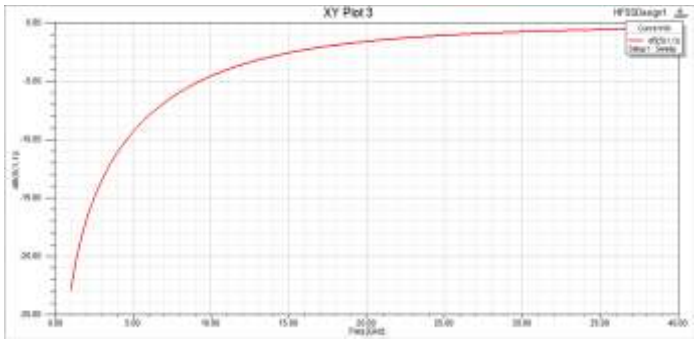

Fig.18 Return loss for Crab-leg flexures beam in upstate position

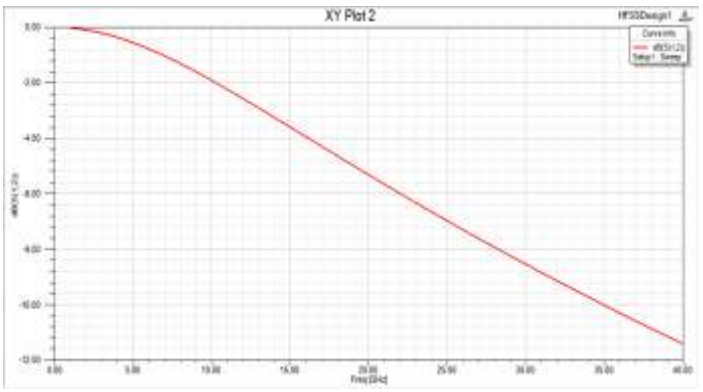

Fig.19 Insertion loss for Crab-leg flexures beam in up-state position

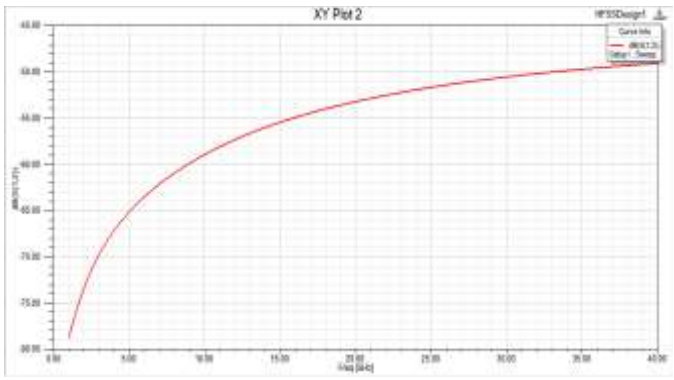

Fig.20 Isolation for Crab-leg flexures beam in down-state position

Table 3: S-parameters for the different beam model

Model	Return loss in dB	Insertion loss in dB	Isolation in dB
Fixed-Fixed	-20 to 16	-0.010 to -0.5	-55 to -60
Fixed-Fixed Flexures	-32 to -26	-0.00 to -0.01	-50 to -55
Crab-leg Flexures	-5 to -4	-0.1 to -0.2	-55 to -65

The table 3 gives the S-parameters for different beam model. When no actuation voltage is applied the S_{11} gives the return loss, S_{12} gives the insertion loss. A low insertion loss is achieved by fixed-fixed flexures beam. When the actuation voltage is applied S_{21} gives the isolation which is better for the crab-leg model.

VI. CONCLUSION

In this work, a RF MEMS Capacitive switch is designed in Coventorware and HFSS for electromagnetic analysis of RF MEMS systems. Using HFSS, RF MEMS shunt switch are analysed, insertion loss, return loss, and isolation loss are studied. Electromagnetic model is extracted from the measured S-parameter. It is seen that insertion loss of capacitive switch is less than -0.2dB for crab-leg flexures beam gives isolation is -65dB for X-band frequency.

REFERENCES

[1] Gabriel M Rebeiz,Jeremy B Muldavin, "RF MEMS Switches and switch circuits," IEEE Microwave Magazine, Dec 2001.

[2] S.K.Lahiri, H. Saha and A.Kundu. "RF MEMS Switch:An Overview ata glance,"International Conference on Computers and Devices for Communication,2009

[3] Jacopo Iannacci, Roberto Gaddi and Antonio Gnudi, "Experimental Validation of Mixed Microelectromechanical and electromagnetic modelling of RF MEMS devices with in a standard IC simulation environment", Journal of Microelectromechanical Systems, vol. 9.No:3 June 2010.

[4] P.D Grant, M.W. Denhoff and R.R.Mansour, "A comparison betweenRF MEMS switches and Semiconductors switch," proceedings of 2004 International Conference on MEMS,NANO and Smart systems,2004.

[5] Jeremy B Muldavin, Gabriel M Rebeiz "Inline Capacitive and DC contact MEMS shunt switches" IEEE Microwave and Wireless Components Letter,vol 11, No 8, August 2001

[6] Jeremy B Muldavin,Gabriel M Rebeiz "High Isolation CPW MEMS Shunt Switches-Part1-Modelling." IEEE Transactions on Microwave Theory and Techniques, Vol 48, No.6, June2000.

[7] Haslina Jaafar, Fong Li Nan, Nurul Amziah Md Yunus " Design and Simulation of High Performance RF MEMS Series Switch.", RSM 2011 Proc.,Kota Kinablu, Malaysia, 2011.

[8] SLucyszyn, S.Pranonsatit, J.Y.Choi, R.W.Moseley, E.M.Yeatman and A.S.Holmes "Novel RF MEMS Switches.", Proceedings of Asia Pacific Microwave Conference ,2007.

[9] Gabriel M Rebeiz "RFMEMS Theory, Design andTechnology.", John Wiley and Sons Limited, New jersey, 2002.

[10] Kenle Chen, Yueyang Dai, Xudong Zou, Jinwen Zhang, "A low loss RF MEMS Switch with dielectric layer on the lower surface of the bridge". Proceedings of 2009 IEEE Conference on NANO/MICRO Engineeredand Molecular Systems, January5- 8 2009.

[11] Jamie Yao, Shea Chen, Susan Eshelman, David Denniston and Chuck Goldsmith "Micromachined Low-Loss Microwave Switches."IEEE Journal of Microelectromechanical Sys tems, Vol.8, No.2, June 1999.

[12] Montserrat Fernandez Bolanos Badia , Elizabeth Buitrago, and Adrian Mihai Ionescu " Rf MEMS Shunt Capacitive Switches Using AlN compared ti Si3N4 Dielectric." Journal of Microelectromechanical Systems, Vol.21, No.5, October 2012.

[13] W.B.Zheng, Q.A.Huang, F.X.Li "Electromagnetic Analysis andFabrication of MEMS Membrane Switches onGaAs Substrates for X-Band Applications." International Conference on Solid State Sensors, Actuators and Microsystems, June 2003

[14] Poonam Verma, Surjeet Singh "Design and simulation of RF MEMS Capacitive type Shunt Switch and its major applications.", IOSR Journal of Electronic Communication Engineering, Vol.4, Jan – Feb 2013

[15] M. Tanga, A.B. Yua, A.Q. Liua,∗, A. Agarwalb, S. Adityaa, Z.S. Liuc"High isolation X-band MEMS capacitive switches" Institute of HighPerformance Computing, Science Park II, Singapore 117528, Singapore Jan 2005

[16] S. Shekhar, K. J. Vinoy, and G. K. Ananthasuresh "Design, Fabrication and Characterization of Capacitive RF MEMS Switches with Low Pull-In Voltage"IEEE 2014

[17] Suparna Sarkar, Dr. A. Vimala Juliet "Design of a Low Voltage RF MEMS Capacitive Switch with Low Spring Constant" Vol. 3, Issue 4, April 2014, IJAREEIE 2014

[18] A. Mahesh, Jyotirmoy Pathak "Thin film Low Voltage RF MEMS Shunt Capacitive Switches Using AIN Dielectric" 2014 IEEE